ANALYSIS OF THE STIMULATION OF A NERVE FIBER SURROUNDED BY AN INHOMOGENEOUS, ANISOTROPIC, AND DISPERSIVE TISSUE

G. D'Inzeo, C. Giacomozzi*, S. Pisa

Department of Electronic Engineering, University of Rome "La Sapienza", Via Eudossiana 18, 00184 Rome, Italy.
*Laboratory of Biomedical Engineering, Istituto Superiore di Sanità, Viale Regina Elena 299, 00161 Rome, Italy.

ABSTRACT

A method for evaluating the threshold for electric and magnetic stimulation of nerves surrounded by an inhomogeneous, anisotropic, and dispersive tissue has been developed. The scalar potential distribution induced by a given electric or magnetic source is evaluated by using the Finite Difference Technique. Calculations are performed with a FORTRAN code, and for non dispersive tissues a spread-sheet is also used. Nerve fiber excitation is described by using the Frankenhaeuser-Huxley model in which the stimulating current density is obtained by extending the method proposed by Rattay. The analysis results predict that, with reference to the homogeneous case usually considered in literature, the larger differences in the current threshold are due to the tissue inhomogeneity, while the consideration of the dispersive properties of the tissues has less effect.

INTRODUCTION

Functional electrical stimulation (FES) is a technique for the rehabilitation of spinal-cord injured patients. It makes use of electrical stimulators to induce currents through the membrane of nerve fibers. These currents trigger action potentials (APs) that propagate along the nerve and induce muscular contraction by means of the synaptic mechanisms still active in paraplegic subjects.

Practical FES realizations concern both upper and lower limbs. For lower limbs Marsolais and Kobetic [1987] have developed a hand-operated stimulator (open loop) that applies trains of biphasic current pulses to the motor point of muscles by using percutaneous intramuscular wire electrodes. Graupe et al. [1988] have realized a closed loop stimulator in which the stimulating current was controlled by the electromiographic (EMG) signal of the upper trunk. Extracutaneous electrodes have been used to stimulate and to measure the response-EMG signal of the stimulated muscles. Paraplegic subjects using this system were able to walk for 300 meters and some of them could climb stairs.

With regard to upper limbs' applications, Buchett et al. [1988] have graded hand movement in quadriplegic subjects by using, as a controller, a shoulder position transducer. The transducer delivers its output to the stimulator module that, in turn, applies current pulses to the muscle by means of percutaneous electrodes. In the controller of their stimulator, Crago et al. [1976] have linearly combined the force and position signals of the hand grasping an object. In this manner and by varying the pulse width of the stimulating current, they could control the finger position, before object acquisition, and both grasp force and opening, after contact.

All the cited authors apply monophasic or biphasic current pulses to the limb to stimulate nerve fibers innervating muscles. For this reason many researchers have studied the threshold response of a nerve fiber to a current signal by introducing different electrical models for the excitation and propagation of the APs.

McNeal [1976] studied the response of a myelinated nerve fiber to a cathodic pulse applied with a spherical electrode. The electrical behavior of the fiber was simulated with a cascade of 11 dipoles (each representing a Ranvier's node) with the central one modelled by means of the Frankenhaeuser-Huxley (F&H) equations [1964]. To evoke an AP with the electrode 1 mm away from the fiber, 100 μs and 226 μA current pulses were necessary. Rattay [1986, 1988, 1989] extended the McNeal's study by considering both myelinated and unmyelinated fibers and electrodes with different geometries. Gorman and Mortimer [1983] analyzed the possibility of a selective excitation of the fibers inside the nerve by varying the electrical parameters of the stimulus. They obtained selectivity by using byphasic stimuli of appropriate widths. Veltink et al. [1989] studied the same problem as a function of the electrode position showing the possibility of selective excitation of the fibers using intraneuronal electrodes.

Nerve stimulation has been also performed by using time varying magnetic fields. This method seems painless compared to the conventional electrical stimulation and, for this reason, has been recently investigated. In particular, Polson et al. [1982], proved experimentally the feasibility of magnetic stimulation of nerve trunks. In their experiments the magnetic field was generated by the discharge through a coil of the charge accumulated on a

capacitor bank. Theoretical investigations have been performed, by using both the F&H [1964] and the Hodgkin-Huxley (H&H) models [1952], to evaluate the threshold of nerve stimulation induced by magnetic fields [Reilly, 1989; Roth and Basser, 1990; Basser and Roth, 1991].
All the quoted authors have studied the action on the nerve of currents flowing through a homogeneous, isotropic, and non dispersive medium. These conditions are never fulfilled practically. The purpose of this work is to develop a method for evaluating the nerve current threshold for electric and magnetic stimulation for the nerve fiber surrounded by an inhomogeneous, anisotropic, and dispersive tissue. The proposed method first evaluates the scalar potential distribution induced by a given electric or magnetic source by using the Finite Difference Technique (FDT) (in the magnetic case, the vector potential distribution is previously evaluated starting from the coil current and position), then it relates the scalar and vector potential distribution along the nerve to the current density crossing the nerve membrane, and finally it computes the nerve response to the resulting current density.
The emphasis in this paper is on the description of the numerical technique used to solve the EM problem, on the characterization of the dispersive properties of the tissue, and on the introduction of a modification of the activating function proposed by Rattay [1986].

METHODS

Finite Difference Technique

FDT has been widely used for studying the scalar potential distribution in a biological tissue due to known electrical [Sowinski and Van Den Berg, 1990; Heringa et al., 1982; Stock et al., 1988] and magnetic sources [Armitage et al., 1983; Gandhi et al., 1984; Polk, 1990; Polk and Song, 1990]. In this section, it will be shown that it is possible, starting from the Maxwell equations, to associate an electrical network with the region under study. The network consists of admittances, whose values are related to the electrical properties of the tissues forming the region, and generators representing the electric and magnetic sources.
To define the electrical network we divide the volume of interest into homogeneous parallelepipedic cells of sides Δx, Δy, Δz centered in (x,y,z) (Fig. 1):

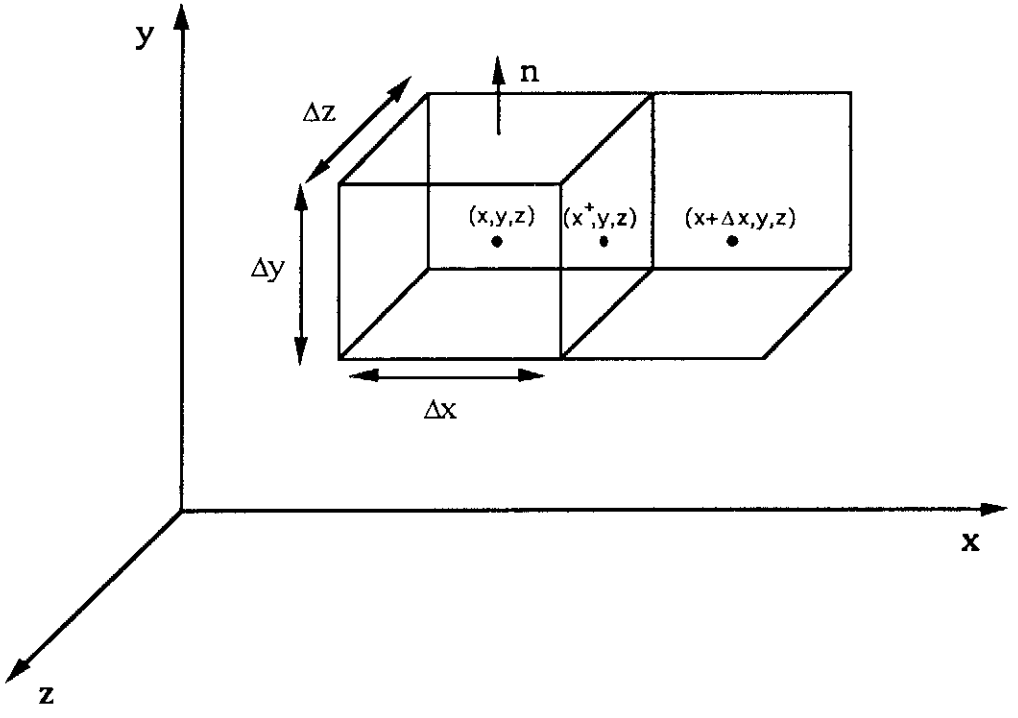

Fig. 1 Unit cell of the FDT lattice.

For each cell we consider the Maxwell equation (assuming harmonic fields):

$$\nabla\times\mathbf{H}= \mathbf{J}_c +\mathbf{J}_d + \mathbf{J}_{ie} = [\sigma]\cdot\mathbf{E} +j\omega[\varepsilon]\cdot\mathbf{E} + \mathbf{J}_{ie} =[\sigma^*]\cdot\mathbf{E} +\mathbf{J}_{ie} \quad (1)$$

where:

$\mathbf{J}_c$ = conduction electric current density,
$\mathbf{J}_d$ = displacement electric current density,
$\mathbf{J}_{ie}$ = impressed electric current density,
$[\sigma]$ = conductivity tensor,
$[\varepsilon]$ = permittivity tensor,
$[\sigma^*]$ = $[\sigma]+j\omega[\varepsilon]$ = complex conductivity tensor.

In the Cartesian coordinates, the conductivity tensor takes the form (in the absence of any static magnetic field):

$$[\sigma^*] = \begin{bmatrix} \sigma_x^* & 0 & 0 \\ 0 & \sigma_y^* & 0 \\ 0 & 0 & \sigma_z^* \end{bmatrix} \tag{2}$$

In eq. (1), the electric field can be expressed in terms of scalar (V) and vector (A) complex potentials as:

$$\mathbf{E} = -j\omega\mathbf{A} - \nabla V \tag{3}$$

Upon taking the divergence of (1), volume integration and subsequent application of the divergence theorem, we obtain:

$$-\oint_S [\sigma^*]\cdot\nabla V\cdot\mathbf{n}\,dS - \oint_S [\sigma^*]\cdot j\omega\mathbf{A}\cdot\mathbf{n}\,dS + \oint_S \mathbf{j}_{ie}\cdot\mathbf{n}\,dS = 0 \tag{4}$$

The FDT consists in approximating the derivatives in (4) by the corresponding incremental ratios, thus obtaining:

$$\begin{aligned} &\sigma_{x^-}^* \frac{(V_{x,y,z}-V_{x-\Delta x,y,z})}{\Delta x}\Delta y\Delta z - \sigma_{x^+}^* \frac{(V_{x+\Delta x,y,z}-V_{x,y,z})}{\Delta x}\Delta y\Delta z + \\ &+ \sigma_{y^-}^* \frac{(V_{x,y,z}-V_{x,y-\Delta y,z})}{\Delta y}\Delta x\Delta z - \sigma_{y^+}^* \frac{(V_{x,y+\Delta y,z}-V_{x,y,z})}{\Delta y}\Delta x\Delta z + \\ &+ \sigma_{z^-}^* \frac{(V_{x,y,z}-V_{x,y,z-\Delta z})}{\Delta z}\Delta x\Delta y - \sigma_{z^+}^* \frac{(V_{x,y,z+\Delta z}-V_{x,y,z})}{\Delta z}\Delta x\Delta y + \\ &+ \sigma_{x^-}^* \Delta y\,\Delta z\, j\omega A_{x^-} - \sigma_{x^+}^* \Delta y\,\Delta z\, j\omega A_{x^+} + \sigma_{y^-}^* \Delta x\,\Delta z\, j\omega A_{y^-} - \sigma_{y^+}^* \Delta x\,\Delta z\, j\omega A_{y^+} + \\ &+ \sigma_{z^-}^* \Delta x\,\Delta y\, j\omega A_{z^-}\,\Delta z - \sigma_{z^+}^* \Delta x\,\Delta y\, j\omega A_{z^+} + I_{ie} = 0 \end{aligned} \tag{5}$$

where I_{ie} represents the impressed current at the node (x,y,z), positive when going out of the cell. The superscripts - and + in the expression mean that the quantity is evaluated on a specific face of the parallelepipedic cell. For example $\sigma_{x^+}^*$ represents the complex conductivity on the face between the cells centered in x and x+Δx (see Fig. 1). Continuity of the complex current at the x^+ surface requires that $\sigma_x^* E_x = \sigma_{x+\Delta x}^* E_{x+\Delta x} = \sigma_{x^+}^* E_{x^+}$, where E_{x+} is given by the negative of the potential gradient in (5) (in the absence of the vector potential and impressed current) and E_x and $E_{x+\Delta x}$ are the x-directed component of the electric fields evaluated, respectively, at x and x +Δx. To satisfy this condition we introduce the complex admittance:

$$Y_{x^+} = (\sigma_{x^+}^*)\frac{\Delta y\cdot\Delta z}{\Delta x} = \frac{2\sigma_x^*\cdot\sigma_{x+\Delta x}^*}{\sigma_x^*+\sigma_{x+\Delta x}^*}\frac{\Delta y\cdot\Delta z}{\Delta x} \tag{6}$$

Similar admittances can be obtained for the other coordinates. With this substitution (5) becomes the Kirchhoff's current equation for an electrical circuit made by a three-dimensional star of admittances and current generators. Fig. 2 shows this circuit for the two-dimensional case.

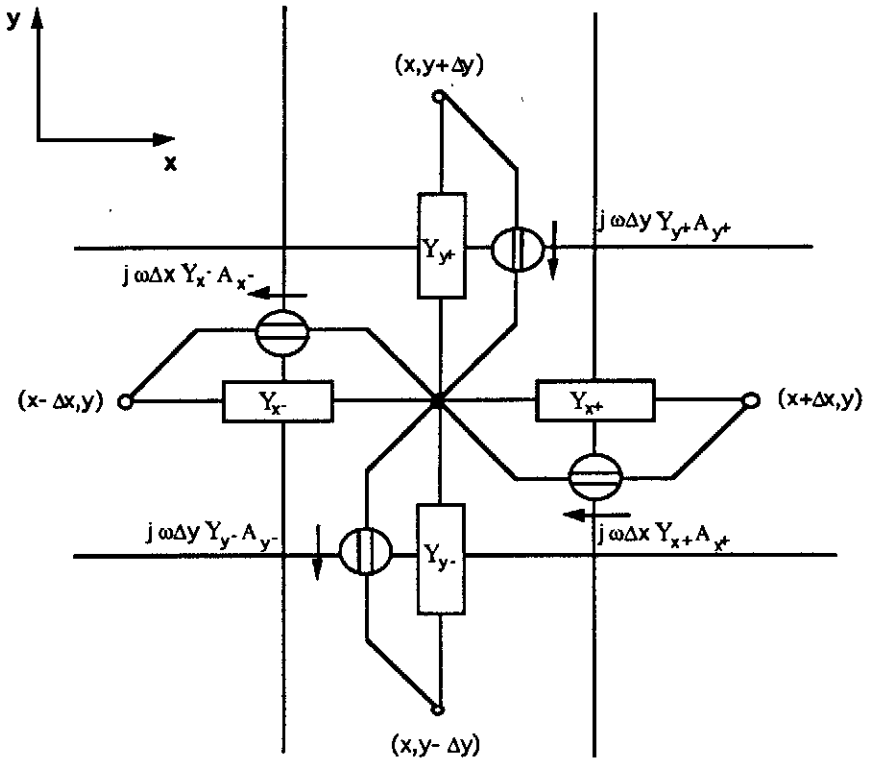

Fig. 2 Two-dimensional representation of the basic circuit.

Both for an electric current stimulation applied directly to nodes, and for a magnetic stimulation applied through an external coil, the potential distribution in the volume of interest can be evaluated by solving a set of simultaneous equations, namely, one per node:

$$V_{x,y,z} = \frac{1}{Y_{x^-} + Y_{x^+} + Y_{y^-} + Y_{y^+} + Y_{z^-} + Y_{z^+}} \cdot [\, Y_{x^+} V_{x+\Delta x,y,z} + Y_{x^-} V_{x-\Delta x,y,z} +$$

$$+ Y_{y^+} V_{x,y+\Delta y,z} + Y_{y^-} V_{x,y-\Delta y,z} + Y_{z^+} V_{x,y,z+\Delta z} + Y_{z^-} V_{x,y,z-\Delta z} +$$

$$- Y_{x^-} \Delta x\, j\omega A_{x^-} + Y_{x^+} \Delta x\, j\omega A_{x^-} - Y_{y^-} \Delta y\, j\omega A_{y^-} + Y_{y^+} \Delta y\, j\omega A_{y^+} +$$

$$- Y_{z^-} \Delta z\, j\omega A_{z^-} + Y_{z^+} \Delta z\, j\omega A_{z^+} - I_{ie}\,] \tag{7}$$

This set of equations is solved using an iterative technique with successive overrelaxation [Ralston and Rabinowitz, 1975]. This technique computes successive estimates of the potential by taking the previous estimate plus a correction term:

$$V^{n+1}(x,y,z) = V^n(x,y,z) + \alpha[V_{x,y,z} - V^n(x,y,z)] \tag{8}$$

where $V^{n+1}(x,y,z)$ and $V^n(x,y,z)$ are the potentials at the (x,y,z) node evaluated at steps n+1 and n respectively, $V_{x,y,z}$ is given by (7) and α is the relaxation constant ($1 < \alpha < 2$). The procedure is terminated when the following criterion is verified:

$$\frac{\sum_{i=1}^{N} |V_i^{n+1} - V_i^n|}{\sum_{i=1}^{N} |V_i^n|} < 0.003 \tag{9}$$

where N is the total number of cells [Veltink et al., 1989].

In the magnetic stimulation we firstly evaluate the vector potential on the cell surfaces, produced by the coil taking into account its position, geometry and current. As reported by Polk [1990], for the frequencies, conductivities, and distances considered in our work ($1 \div 10^6$ Hz; $0.013 \div 0.5$ S/m; $1 \div 100$ mm), we can apply the quasi-static approximation, and the vector potential can be expressed as:

$$\mathbf{A} = \frac{\mu}{4\pi}\iiint \frac{\mathbf{J}_i dv}{R} \tag{10}$$

where $\mathbf{J}_i$ represents the volume current density that flows in the coil and produces the magnetic field. The vector potential at the center point of the cell surfaces is evaluated by approximating the coil with a 64-sided polygon and summing the contributions of each side [Roth and Basser, 1990]. Starting from the value of the vector potential on the cell surfaces it is possible to evaluate the intensity of the current generators (Fig. 2). Finally eq. (7) is iterated up-to convergence.

Cross-Sectional Geometry and Electrical Properties of the Forearm

In our study we model the stimulation of the right forearm cutaneous nerve "antebrachii medianus" at the level of the third proximal. This nerve is not usually stimulated for rehabilitation purposes and it is chosen just to show the technique.

To identify the cell grid for the FDT, the cross-sectional anatomical picture of the right forearm at the level of the third proximal, reported in Sobotta and Becher [1983], is digitized into a computer by using a scanner (PC Scan 1000 DEST) with a resolution of 300 pixels per inch. The section is then subdivided into 30x25 square cells of 3mm side, each homogeneously filled with the prevailing tissue (Fig. 3).

In the three-dimensional study we consider parallelepipedic cells of 3x3x2mm sides. For each cell, the longitudinal dimension (2mm) is chosen to correspond to the internodal distance in myelinated fibers and it allows us to evaluate, by using the FDT, the scalar potential for Ranvier's nodes [McNeal, 1976]. The forearm structure is assumed to be cylindrical and it is obtained by superimposing a given number of parallelepipedic cell layers.

With each cell we associate a conductivity and a permittivity that, in some cases, are different in the transverse and longitudinal directions (anisotropic tissues). The conductivity values are taken from various experimental reports [Geddes and Baker, 1967; Stuchly and Stuchly, 1980; Polk and Postov, 1986]. For the permittivity we consider the frequency dependence, and use the analytical expression for the permittivity to interpolate the experimental data from Polk and Postow [1986] (see third and fifth column of Table I). The interpolating function gives a good fit of the experimental data for frequencies from dc to about 10MHz.

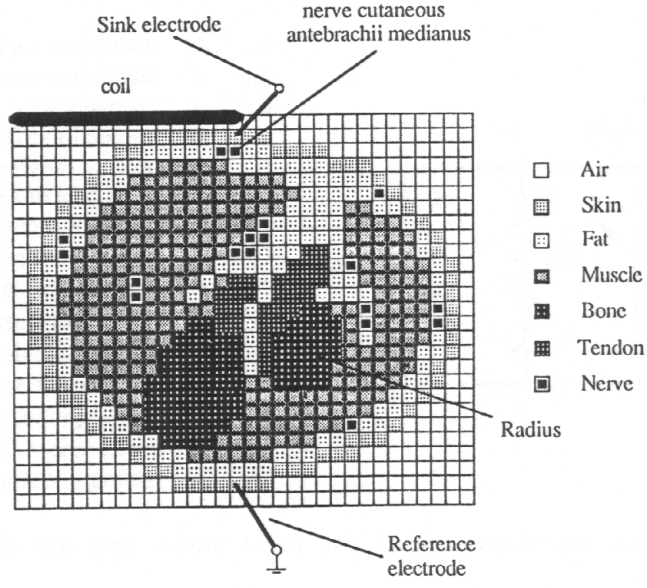

Fig. 3 Diagram of the forearm cross-section.

Biological Tissue		Transversal Conductivity σ_t (S/m)	Transversal Permittivity ε_{Rt}	Longitudinal Conductivity σ_z (S/m)	Longitudinal Permittivity ε_{Rz}
Air	0	0.0	1.0	0.0	1.0
Skin	1	0.5	$10^{6.5-0.5\text{Log}_{10}(f+1)}$	0.5	$10^{6.5-0.5\text{Log}_{10}(f+1)}$
Fat	2	0.05	$10^{6-0.5\text{Log}_{10}(f+1)}$	0.05	$10^{6-0.5\text{Log}_{10}(f+1)}$
Muscle	3	0.08	$10^{8-0.75\text{Log}_{10}(f+1)}$	0.5	$10^{6.5-0.5\text{Log}_{10}(f+1)}$
Bone	4	0.013	$10^{4-0.33\text{Log}_{10}(f+1)}$	0.013	$10^{4-0.33\text{Log}_{10}(f+1)}$
Tendon	5	0.013	$10^{4-0.33\text{Log}_{10}(f+1)}$	0.013	$10^{4-0.33\text{Log}_{10}(f+1)}$
Nerve	6	0.05	$10^{6-0.5\text{Log}_{10}(f+1)}$	0.5	$10^{6-0.5\text{Log}_{10}(f+1)}$

Table I

Modeling of Nerve Fiber Excitation

The nerve model used to evaluate the threshold response of the fiber is that of Frankenhaeuser and Huxley (F&H) [1964] (Fig. 4). The stimulating current density in this model is evaluated extending the method proposed by Rattay [1989]. Rattay showed that, in simulating the stimulation of a nerve fiber with external electrodes, the current density used in the F&H model is proportional to the longitudinal derivative, evaluated at the node of Ranvier, of the longitudinal component of the electric field.

Because of the dispersive properties of the tissues the scalar potential at each point inside the forearm varies with the frequency of the stimulating current. For this reason we introduce in the frequency domain a complex transfer function T(f) defined, at each frequency, as the ratio between the current density stimulating the nerve ($J_S(f)$) and the applied electrode current (I_e). Extending the Rattay model in the frequency domain this ratio can be expressed as a function of the scalar and vector potential distribution along the nerve:

$$T(f) = \frac{J_S(f)}{I_e} = \frac{d\,\Delta z}{4\,\rho_i\,L\,I_e} \cdot \left\{ \frac{V_{z-\Delta z}(f) - 2V_z(f) + V_{z+\Delta z}(f)}{\Delta z^2} + j\omega \frac{A_{z'} - A_z}{\Delta z} \right\} \quad [m^{-2}] \qquad (11)$$

To evaluate the time behavior $J_S(t)$ of the stimulating current density, first we apply the Fourier-transform to the electrode current, then the obtained frequency spectrum is multiplied by T(f), and, finally, the inverse Fourier transform of the result gives the time behavior of the current density $J_S(t)$ used in the F&H model.

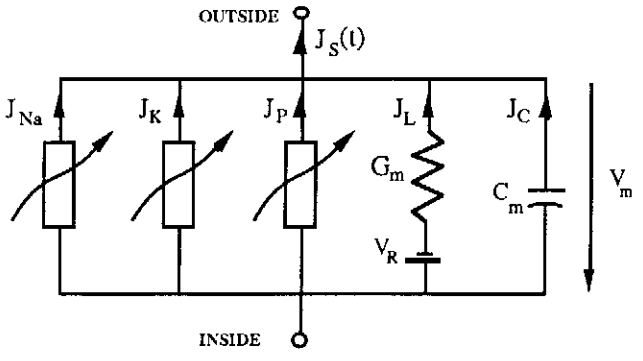

c_m = membrane capacitance / unit area
g_m = membrane conductance / unit area
d = axon diameter
ρ_i = intracellular fluid resistivity
L = node of ranvier width
Δz = internodal distance
C_m = $c_m \pi dL$ = membrane capacitance
G_m = $g_m \pi dL$ = membrane conductance
J_{NA} = sodium current density
J_K = potassium current density
J_P = non specific delayed current density
J_L = leak current density
J_I = $J_{NA}+J_K+J_P+J_L$
V_m = membrane voltage
V_R = resting potential

Fig. 4 Equivalent circuit representation of the F&H model and list of symbols used.

The time behavior of the membrane voltage V_m in response to the stimulating current density is evaluated by solving the differential equation:

$$\frac{dV_m}{dt} = \frac{1}{c_m}\left[-J_I(t) + J_S(t)\right] \tag{12}$$

Four additional differential equations with nonlinear coefficients are necessary to evaluate $J_I(t)$ [Frankenhaeuser and Huxley, 1964]. This set of five differential equations has been solved by using the Runge-Kutta numerical method [Ralston and Rabinowitz, 1975]. As an example Fig. 5 shows the time behavior of the membrane voltage in response to 120μs current density pulses with different amplitudes. The figure shows that excitation occurs for amplitudes above 775 μA/cm^2 with the considered signal.

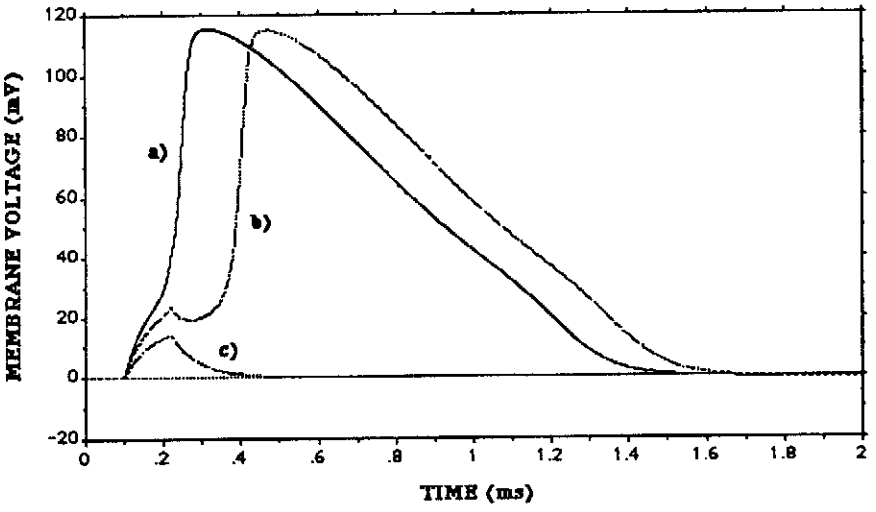

Fig. 5 Time behavior of the membrane voltage in response to 120μs current density pulses with different amplitudes; a) 1000μA/cm^2, above threshold response; b) 775μA/cm^2, threshold response; c) 500μA/cm^2, subthreshold response.

FDT Solution Methods

The electromagnetic problem is numerically solved using a FORTRAN code. For non dispersive tissues, both a FORTRAN code and a spread-sheet (Wingz™) are used. Spread-sheets have already been introduced in the past to get iterative solutions of finite difference problems [Hart, 1989a, 1989b, 1990]. In this work the spread-sheet Wingz™ has been chosen for its capability of managing a large number of cells simultaneously, and because of its excellent graphic capabilities. In the application of the spread-sheet to solve the FDT problem, we first fix the number of transverse sections of the forearm to be considered, then, for each section, three regions of 30x25 cells are defined on the spread-sheet. The conductance values of the forearm cells are inserted in each cell of the first region; in the cells of the second section we place, in the electrical stimulation the sink and references current values, and in the magnetic stimulation, the sum of the currents of the generators dependent on the vector potential. Starting from the knowledge of conductivity and electrode matrices it is possible to implement Eq. (7) in a cell of the third region and to copy it into all the remaining cells. To find a solution of the problem, the iterative technique is applied by using the spread-sheet property of calculating a new value in a specific cell whenever a variation takes place in one of the adjacent cells. It must be noted that a further aid to the implementation of this procedure is provided by the possibility of programming the spread-sheet Wingz™. It uses a high-level programming language, and the calculations can be executed automatically.

As an example, let us consider a forearm model obtained by superimposition of five sections, that is 3750 grid points. By considering an electrical stimulation (f = 0) with a relaxation constant α=1.5, the convergence criterion (9) is reached after 225 iterations. This number corresponds to an execution time of 70 minutes on a Macintosh SE/30. The same time is necessary to solve the problem with the FORTRAN program on the same computer.

RESULTS

Electrical Stimulation

The electrical stimulation is performed by placing the electrodes on a transverse section of the forearm. The sink electrode is placed on the skin, 3mm from the cutaneous nerve 'antebrachii medianus'; the reference electrode is placed on the other side of the forearm (Fig. 3). The stimulating signal with a pulse width of 120μs and a slew-rate of 1mA/μs is shown in Fig. 7a. The pulse amplitude (I_P) is evaluated as the threshold value (current threshold) necessary to obtain the excitation of the nerve membrane, that is a stimulating current density amplitude of 775 $\mu A/cm^2$ (threshold current density).

In the following study, three cases will be evaluated:

a) homogeneous and non dispersive,

b) inhomogeneous and non dispersive,

c) inhomogeneous and dispersive.

In a) the forearm tissue is assumed homogeneous with a conductivity of 0.08 S/m that corresponds to the transverse conductivity of the muscle (see Table I); in b) the inhomogeneities of the forearm are considered and for each tissue the conductivity values shown in Table I are used; finally in c) the permittivity of the forearm tissues is introduced and its frequency dependent behavior is considered as given by the analytical expressions in Table I. The c) situation is the real one, however, the a) and b) cases are analyzed to show the effect of the subsequent approximations on the current threshold.

a) homogeneous and non dispersive. In this situation the scalar potential inside the forearm does not vary with the frequency of the electrode current. The electromagnetic problem is solved in the f=0 case (no vector potential) and by considering five longitudinal layers of parallelepipedic cells.

The transfer function T(f) is evaluated using Eq. (11). It can be noted that by using the FDT the potential is calculated apart from an additive term that can be ignored since, to compute the transfer function only differences of potential are considered. Since T(f) is frequency independent, the stimulating current density is simply proportional to the electrode current. By applying this current density to the F&H model a current threshold value of 65μA is obtained. This value is close to that found by using, for the evaluation of the potential, the equation: $V_e=\rho_e I_{ie}/4\pi R$ where I_{ie} is the electrode current, ρ_e the tissue resistivity, and R the distance between the electrode and the nerve [Rattay, 1986]. From this equation evaluated for R=3mm, a current threshold of 100μA is found. In our simulation we obtain a lower current threshold since the current does not flow in all the directions but only in a confined region (Fig. 6a), so for the same electrode current the voltage gradient and the corresponding stimulating current density are higher.

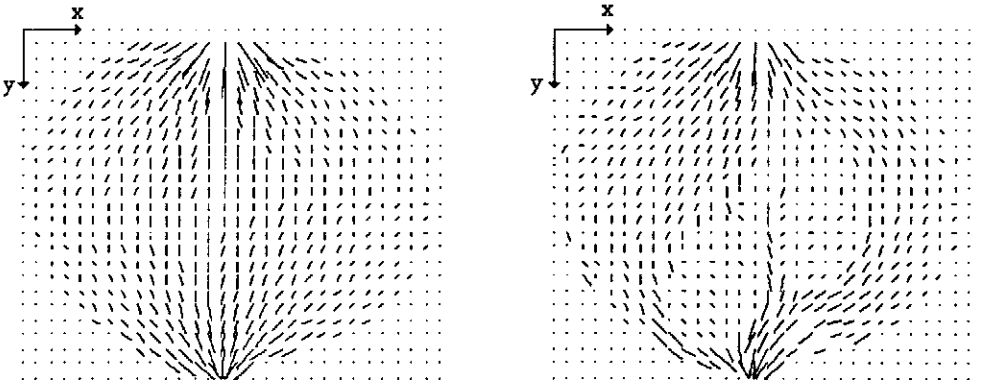

Fig. 6 Current density in the central layer of the forearm for the homogeneous and non dispersive tissue (a), and for the inhomogeneous and non dispersive tissue (b).

b) inhomogeneous and non dispersive. The effects of the tissue inhomogeneities on the current density distribution are evidenced in Fig. 6b. Low current values inside the low conductance tissues (bone and tendon in Fig. 3) can be seen. In this situation, the transfer function is still constant with frequency, but 20 times lower than in a). Higher pulse amplitudes are necessary to evoke an action potential (I_p=1.22 mA with 5 layers).

c) inhomogeneous and dispersive. In this case the potential and T(f) vary with frequency. The stimulating current density is obtained by using the technique previously described for the dispersive case. By applying the electrode current shown in Fig. 7a we obtain the stimulating current density $J_S(t)$ shown in Fig. 7b. In spite of the difference in signal shape, the current threshold does not change very much (1.20 mA with 5 layers) with respect to the non dispersive case b). A time behavior similar to that reported in Fig. 7b has been experimentally obtained for upper limbs [McGill et al., 1982].

The performed analysis shows that, with reference to the homogeneous case, usually considered in literature, the most important differences are due to the tissue inhomogeneity, while the non dispersive tissue hypothesis does not cause significant errors. Since Wingz™ can be used only for the nondispersive case, the obtained results suggest that the spread-sheet is a very useful tool for this kind of application.

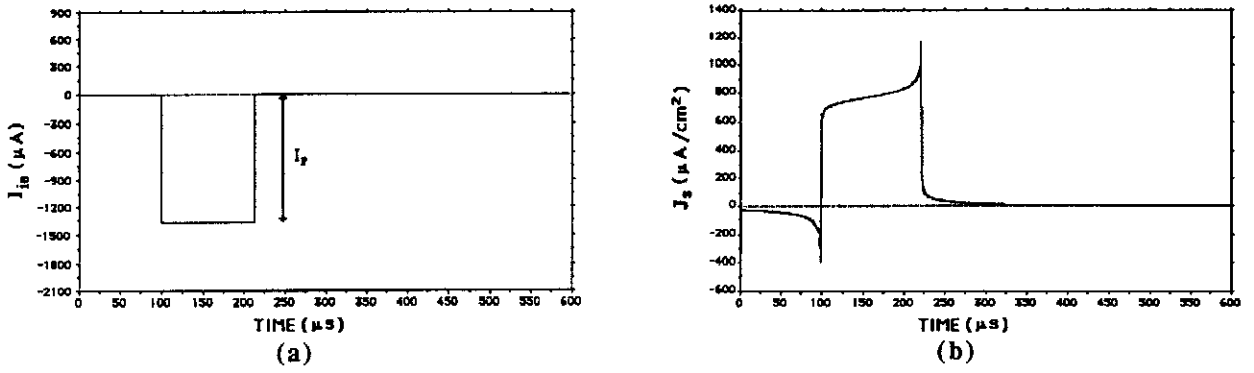

Fig. 7 Time behavior of the input electrodic current (a) and of the stimulating current density (b) evaluated in the dispersive case.

Magnetic Stimulation

As in the electric situation, also in the magnetic one, stimulation of the nerve 'antebrachii medianus' will be modeled. The stimulation is obtained by a 30 turn external circular coil having a radius of 2.4 cm (L=0.165mH, R=3Ω) placed 3mm from the forearm (Fig. 3) [Roth and Basser, 1990]. The coil current is generated by the discharge of a capacitance (C=300μF) initially at a voltage V_0. The time behavior of the coil current is:

$$I_c(t) = \frac{V_0}{\sqrt{\left(\frac{R}{2}\right)^2 - \left(\frac{L}{C}\right)}} \exp\left(-\frac{R}{2L}t\right) \sinh\left(\sqrt{\left(\frac{R}{2L}\right)^2 - \left(\frac{1}{LC}\right)}\ t\right) \qquad (13)$$

Since in eq. (13) all the parameters are fixed except the voltage V_0, we relate the stimulation of the nerve membrane to this parameter (voltage threshold).

In the magnetic stimulation we will analyze two situations for the forearm tissue:

a) homogeneous and non dispersive,

b) inhomogeneous and dispersive.

a) homogeneous and non dispersive. In this situation the vector potential in eq. (11) is evaluated by eq. (10). By solving this problem, we found that scalar potential values give a negligible contribution to the T(f). The small scalar potential values depend on the homogeneous tissue assumption; in this case, in fact, there is no charge accumulation at the boundaries between different tissues. To further reduce the boundary effect due to the longitudinal truncation of the forearm, we have increased the number of cell layers to 49. Fig. 8a shows the transfer function (f=50 Hz) on a plane containing the nerve and parallel to the coil surface. The maximum of T(f) corresponds to the point of the nerve that will be excited with the lowest voltage. By shifting the coil center with respect to the nerve by a distance equal to the coil radius the higher current density value is obtained at the nerve position. Fig. 8b shows T(f) (obtained as in Fig. 8a) in a transverse plane 24 mm from the central layer. The figure shows that, as in the electrical case, the points with highest current density are those close to the skin and the current density decreases by increasing the distance from the skin. In the magnetic stimulation, however, the region with high current density is larger than for the electric case.

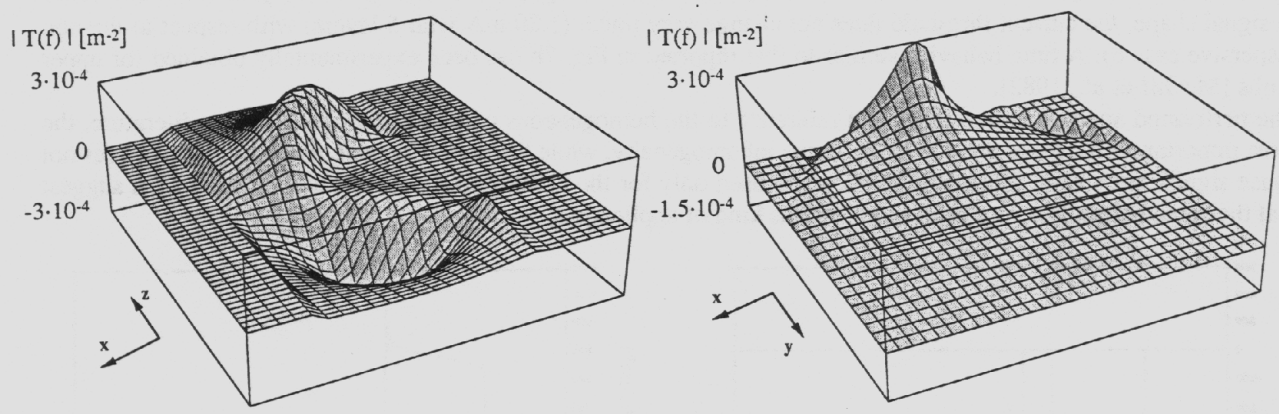

(a) (b)

Fig. 8 Transfer function on a plane parallel (a) and transverse (b) to the coil surface.

Since the vector potential gives the main contribution to the transfer function T(f), the stimulating current density is practically related only to the time derivative of the coil current I_C (a multiplication factor $j\omega$ in the frequency domain corresponds to a derivative in the time domain).

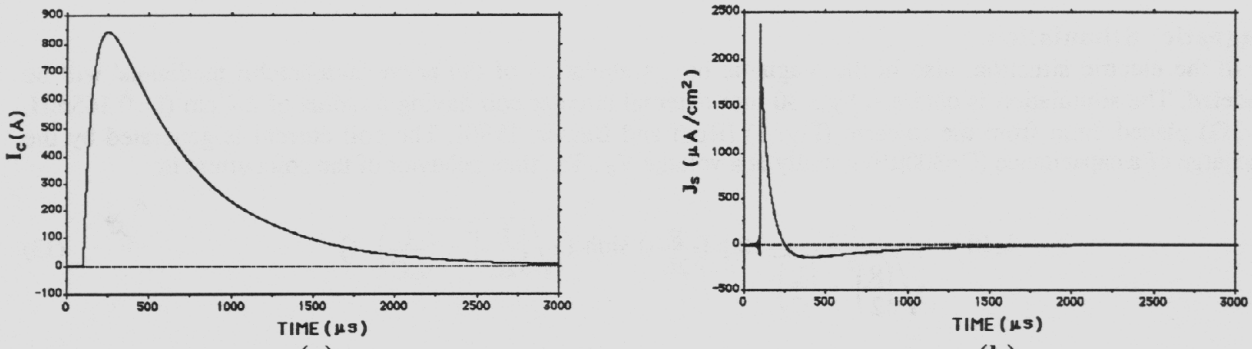

(a) (b)

Fig. 9 The coil current (a) and the stimulating current density (b).

Fig. 9 shows the time behavior of the current in the coil (a) and of the stimulating current density (b). These figures are obtained by applying a voltage V_0 of 3250 Volts that represents the voltage threshold for this situation. By using a model of the mammalian myelinated axon and lightly different coil parameters, Basser and Roth [1991] obtained voltage threshold values of the same order of magnitude.

b) inhomogeneous and dispersive: By considering the dispersive and inhomogeneous properties of the tissue of the forearm, the scalar voltage gives a contribution to the transfer function that is opposite to the vector potential one and it causes a reduction in the T(f) values and consequently an increase in the coil current necessary to excite the nerve. In this situation we observe a 40% increase in the voltage on the capacitance necessary to evoke a spike on the nerve (V_0 = 4700 Volts). The obtained values for the voltage on the capacitance are similar to those found experimentally by Polson et al. [1982]. An exact comparison with the Polson data is not possible since the distance between the coil and the nerve is not reported.

CONCLUSION

The proposed technique allows to study the threshold for electric and magnetic nerve stimulation by assuming the nerve fiber surrounded by an inhomogeneous, anisotropic and dispersive tissue. The study shows the importance of considering the tissue inhomogeneities for evaluating the threshold, while, in the cases examined, the dispersive properties of the tissue are less important. The proposed method can be used both for the analysis and the synthesis of FES stimulators, as well as for the study of multi-electrode configurations. To improve the technique, a reduction of the cell dimensions should be considered. For the same anatomical section, this reduction causes an increase in the computation time and necessary computer memory. With modern computers, and in view of the small memory occupations by the FDT used in the present study, it should be possible to extend the technique. Another improvement can be obtained by considering a more realistic anatomical picture of the forearm.

REFERENCES

Armitage D. W., H. H. Leveen, R. Pethig (1983), Radiofrequency-Induced hyperthermia: Computer Simulation of Specific Absorption Rate Distribution Using Realistic Anatomical Models, Phys. Med. Biol, 28: 31-42.

Basser P. J., B. J. Roth (1991), Stimulation of a Myelinated Nerve Axon by Electromagnetic Induction, Med. & Biol., Eng. & Comput, 29: 261-268.

Buckett J. R., P. H. Peckham, G. B. Thrope, S. D. Braswell, M. W. Keith (1988), A Flexible, Portable System for Neuromuscular Stimulation in the Paralyzed Upper Extremity, IEEE Trans. Biomed. Eng., 35 (11): 897-904.

Crago P. E., R. J. Nakay, H. C. Chizeck (1976), Feedback Regulation of Hand Grasp Opening and Contact Force During Stimulation of Paralyzed Muscle, IEEE Trans. Biomed. Eng., 38 (1): 17-28.

Frankenhaeuser B., A. F. Huxley (1964), The Action Potential in the Myelinated Nerve Fiber of Xenopus Laevis as Computed on the Basis of Voltage Clamp Data, J. Physiol.,171: 302-315.

Gandhi OM P., J. F. De Ford, Hiroshi Kanay (1984), Impedence Method for Calculation of Power Deposition Patterns in Magnetically Induced Hypertermia, IEEE Trans. Biomed. Eng., 31 (10): 644-651.

Geddes L. A., L. E. Baker (1967), The Specific Resistance of Biological Material a Compendium of Data for the Biomedical Engineer and Physiologist, Med. & Biol., Eng. & Comput, 5: 271-293.

Gorman P. H., J. T. Mortimer (1983), The Effect of Stimulus Parameter on the Recruitment Characteristics of Direct Nerve Stimulation, IEEE Trans. Biomed. Eng., 30 (7): 407-414.

Graupe D., K. H. Kohn, S. Bassens (1988), Above and Below-Lesion EMG Pattern Mapping for Controlling Electrical Stimulation of Paraplegics to Facilitate Unbraced Walker-Assisted Walking, Journal of Biomed. Eng., 10: 305-311.

Hart F. X. (1989a), Using a Spreadsheet Program to Model the Interaction of Low-Frequency Electric Fields with Inhomogeneous Irregularly Shaped Objects, Journal of Bioelectricity, 8 (2): 201-226.

Hart F. X. (1989b), Validating Spreadsheet Solutions to Laplace's Equation, Am. J. Phys., 57 (11): 1027-1034.

Hart F. X. (1990), Use of a Spreadsheet to Calculate the Current Density Distribution Produced in Human and Rat Models by Low-Frequency Electric Fields, Bioelectromagnetics, 11: 213-228.

Heringa A., D. F. Stegeman, G. J. H. Uijen, J. P. C. De Weerd (1982), Solution Methods of Electrical Field Problems in Physiology, IEEE Trans. Biomed. Eng., 29 (1): 34-42.

Hodgkin A. L., A. F. Huxley (1952), A Quantitative Description of Membrane Current and its Application to Conduction and Excitation in Nerve, J. Physiol., 117: 500-544.

Marsolais E. B., R. Kobetic (1987), Functional Electric Stimulation for Walking in Paraplegia, The Journal of Bone and Joint Surgery, 69-A (5): 728-733.

McGill K. C., K. L. Cummins, L. J. Dorfman, B. B. Berlizot, K. Luetkemeyer, D. G. Nishimura, B. Widrow (1982), On the Nature and Elimination of Stimulus Artifact in Nerve Signal Evoked and Recorded Using Surface Electrodes, IEEE Trans. Biomed. Eng., 29 (2): 129-137.

McNeal D. R. (1976), Analysis of a Model for Excitation of Myelinated Nerve, IEEE Trans. Biomed. Eng., 23 (4): 329-336.

Polk C., E. Postow (1986), CRC Handbook of Biological Effects of Electromagnetic Fields, CRC Press.

Polk C. (1990), Electric Fields and Surface Charges Induced by ELF Magnetic Fields, Bioelectromagnetics, 11: 189-201.

Polk C., J. H. Song (1990), Electric Fields Induced by Low Frequency Magnetic Fields in Inhomogeneous Biological Structures that are Surrounded by an Electric Insulator, Bioelectromagnetics, 11: 235-249.

Polson M. J. R., A. T. Barker, I. L. Freeston (1982), Stimulation of nerve trunks with time-varying magnetic fields, Med. & Biol., Eng. & Comput, 20: 243-244.

Ralston A., P. Rabinowitz (1975), A first course in numerical analysis, New York: McGraw-Hill

Rattay F. (1986), Analysis of Models for External Stimulation of Axons, IEEE Trans. Biomed. Eng., 33 (10): 974-977.

Rattay F. (1988), Modeling tha Excitation of Fibers Under Surface Electrodes, IEEE Trans. Biomed. Eng., 35 (3): 199-202.

Rattay F. (1989), Analysis of Models for Extracellular Fiber Stimulation, IEEE Trans. Biomed. Eng., 36 (7): 676-682.

Reilly J. P. (1989), Peripheral Nerve Stimulation by Induced Electric Currents: Exposure to Time-Varying Magnetic Fields, Med. & Biol., Eng. & Comput, 27: 101-110.

Roth B. J., P. J. Basser (1990), A Model of the Stimulation of a Nerve Fiber by Electromagnetic Induction, IEEE Trans. Biomed. Eng., 37 (6): 588-597.

Sobotta J., H. Becher (1983), Atlante di Anatomia dell'uomo, ed. USES.

Sowinski M. J., P. M. Van Den Berg (1990), A Three Dimensional Iterative Scheme for an Electromagnetic Capacitive Applicator, IEEE Trans. Biomed. Eng., 17 (10): 975-986.

Stok C. J., M. Petronella, A. Wognum (1988), A Noniterative Approximate Solution Method for Volume Conductor Problems Based on the Finite Difference Method, IEEE Trans. Biomed. Eng., 35 (1): 31-35.

Stuchly M. A., S. S. Stuchly (1980), Dielectric Properties of Biological Substances - Tabulated, J. of Microwave power, 15 (1): 19-26.

Veltink P. H., B. K. Van Veen, J. J. Struijk, J. Holsheimer, H. B. K. Boom (1989), A Modeling Study of Nerve Fascicle Stimulation, IEEE Trans. Biomed. Eng., 36 (7): 683-692.